

2-step 공정법에 의해 상온 증착된 ITO박막의 전기 광학적 특성 향상

김종훈, 안병두, 전경아, 강홍성, 이상렬
연세대학교

Enhancement in electrical and optical properties of ITO thin films grown by 2-step process at room temperature

Jong Hoon Kim, Byung Du Ahn, Kyung Ah Jeon, Hong Seong Kang, and Sang Yeol Lee
Yonsei University

Abstract - The optical and electrical properties of indium tin oxide (ITO) thin films deposited at room temperature can be substantially enhanced by adopting a two-step process. In the first step, the films (50 nm thick) were grown by pulsed laser deposition (PLD) on glass substrate at room temperature and quickly annealed at 400°C in nitrogen ambient for 1 minute by using rapid thermal annealing method. The process was completed by additional deposition (150 nm thick) on annealed film at room temperature. High quality ITO films grown by two-step process at room temperature could be obtained with the resistivity of $3.02 \times 10^{-4} \Omega\text{cm}$, the carrier mobility of $32.07 \text{ cm}^2/\text{Vs}$, and the transparency above 90 % in visible region mainly due to the enhancement of the film crystallinity and the increase of grain size.

1. Introduction

Indium tin oxide (ITO) is widely used as a transparent electrode in optoelectronic devices because the films have high transmittances in the visible region and low resistivity. It is well known that the low resistivity value of ITO films is due to a high carrier concentration caused by both oxygen vacancies and substitutional tin dopants. Also, the high transparency in the visible and near-IR region is caused by the wide band gap.

In this paper, we report the enhancement of the electrical, structural, and optical properties of ITO thin films prepared at room temperature by using the new two-step process with PLD.

2. Experimental

The amorphous ITO thin films were deposited at room temperature by using PLD with a Nd:YAG laser (355 nm, 5 Hz, and FWHM of 6 nm) with a thickness of 50 nm in the first step. The target used in this study was a sintered ITO pellet containing 5 wt. % SnO_2 . The ablated material was deposited on $1.25 \times 1.25 \text{ cm}^2$ glass substrates (microscope cover glass, Marienfeld). The substrates were ultrasonically cleaned in acetone and methanol, rinsed in deionized water, and subsequently dried in a flowing nitrogen gas before deposition. The basal vacuum in the chamber was as low as 10^{-6} Torr. The target was rotated at 4 rpm to preclude pit formation and to ensure uniform ablation of the target. The laser energy density on the target was 2.0 J/cm^2 , and the

target-substrate distance was 5 cm. Oxygen gas was injected into the chamber by using a mass flow controller to create a pressure of 15 mTorr. After the first deposition, ITO films were annealed by rapid thermal annealing (RTA) in nitrogen ambient (760 Torr) at 400°C for 1 min to improve crystallinity. The two-step processed ITO film was completed by a second deposition on the annealed crystalline ITO film with a thickness of 150 nm and with a laser repetition rate of 1 and 5 Hz respectively. Other growth conditions are the same as the first deposition.

3. Result and discussion

To observe the effect of the two-step process, samples were prepared in 4 different conditions. All films were grown by PLD on glass with a thickness of 200 nm. Sample A is the as grown ITO film deposited at room temperature. Sample B is the film deposited at room temperature and annealed by RTA in nitrogen ambient (760 Torr) at 400°C, for 1 min. Sample C and D are two-step processed ITO films with the laser repetition rate of 1 and 5 Hz in the second deposition, respectively. Figure 1 illustrates the variation of resistivity, carrier density, and Hall mobility as a function of processing conditions. It has been observed that the electrical properties are strongly influenced by the processing condition. Relative high resistivity of $1.23 \times 10^{-3} \Omega\text{cm}$ was obtained from as-grown sample (Sample A) and it decreased to a lower value of 9.19×10^{-4} and $3.02 \times 10^{-4} \Omega\text{cm}$ from Sample B and C, respectively. This decrease in resistivity may be due to the reduction of severe oxygen deficiencies which cause the lattice structural disorders (see Fig. 2) and consequently reduce the mobility of carriers, by RTA treatment[1].

The resistivity of Sample B is higher than that of Sample C. This may have been caused by the fact that the RTA time of 1 minute is enough to crystallize the buffer layer with the thickness of 50 nm, but not enough for entire films. In the case of Sample D, high resistivity of $1.30 \times 10^{-3} \Omega\text{cm}$ was observed. It is suggested that the laser repetition rate of 5 Hz is too fast to keep the ordinary arrangement of the film, because of overstacking during the second deposition.

This variation in resistivity may be due to different grain sizes [2]. AFM measurement indicates that the grain size of the films changes by varying the processing conditions [3]. The AFM image of Sample

A shows a very smooth surface with an rms roughness of 5.2. On Sample C, the rms roughness increases to 24.8 because of the enhancement of crystallinity. A larger grain size results in lower density of grain boundaries, which behave as traps for free carriers and barriers for carrier transport in the film. Thus, the decrease in resistivity is accompanied by the increase in both the Hall mobility and the carrier density of the films, which result from the increased grain size.

Moreover, the two-step process enhances crystallinity of the films (see Fig. 2). In ITO films, Sn atoms in crystal lattices (so called 'activated Sn atoms') generate carrier electrons. On the contrary, since Sn atoms in the amorphous ITO grains were not activated, they do not make carriers but neutral scattering centers, such as SnO_x clusters [4].

Figure 2 represented the XRD patterns of ITO films as a function of processing conditions. To compare the intensity of each film, the Y-axis was fixed with the same scale. It can be seen that X-ray diffraction patterns of as grown ITO film (Sample A) did not show any peak, suggesting an amorphous layer. However, the structure of the ITO film became a crystalline one after RTA or the two-step process. On Sample B and C, the intensities of the major (222) peak of the ITO films increased significantly and its value of full width at half maximum (FWHM) was 0.32 and 0.22, respectively. It is well agreed with the result of electrical properties as mentioned in Fig. 1. However, the peak intensity was reduced and (222) peak splitted into two peaks in the case of Sample D. Izumi group reported a similar peak split observed in sputtered ITO films and proposed the residual stress model [5]. In our case, it is suggested that the development of the intrinsic stress in the film appeared to have been caused by the overstacking during the second deposition with a repetition rate of 5 Hz.

The effect of processing condition on the optical properties of ITO films is shown in Fig. 3. It is known that the increase in optical transmittance can be attributed to the improvement of crystallinity and stoichiometry [6]. High transmittance (above 90 %) in the visible region was exhibited from Sample B and C. This high transmittance may be due to the enhancement of the crystallinity and stoichiometry of the ITO films and it is well agreed with the electrical and structural properties illustrated in Fig. 1 and 2, respectively. On Sample A, the transmittance is relatively low because the crystallization energy is not sufficient to form a stoichiometric film.

The inset of Fig. 3 shows the variation of the optical band gap energy as a function of processing condition. The optical band gap could be obtained from the intercept of α^2 (α : absorption coefficient) versus $h\nu$ for direct allowed transitions. The value of the optical band gap is observed to vary from 3.76 (Sample A) to 4.13 eV (Sample C). The change of optical band gap can be explained by Burstein-Moss shift [7]. This increase in the band gap is due to the increase in free electron concentration in the films evidenced in Fig. 1. It is the result of a large increase in the free carrier concentration and the corresponding upward shift of the Fermi level to the top of the band edge. Generally, it is well known that the broadening

in absorption edge is mainly due to the increase of disorders in semiconductor films, which lead to the appearance of localized electron and/or hole states [8]. Sample A shows broader absorption edge compared to Sample C, and this result also supports the electrical and structural properties of these films mentioned in Fig. 1 and 2.

As mentioned in Fig. 1, there are two main reasons of carrier generation in ITO films; native oxygen vacancies and substitutional tin dopants. The oxygen vacancies create free electrons in the films because one oxygen vacancy creates two extra electrons in the films. And Sn atoms which substituted in sites in crystal lattices generate carrier electrons. These two factors are in trade-off. Both relatively low resistivity and high electron mobility were consistent with the enhancement of optical transmittance in our two-step processed crystalline ITO films.

4. Conclusion

In summary, we have suggested a new process to enhance the properties of ITO thin films. By using the two-step process, films have larger grain size and better crystallinity which is the origin of the enhancement of the electrical and optical properties. High quality ITO films with a resistivity of $3.0210^{-4} \Omega \square$, a carrier mobility of $32.07 \text{ cm}^2/\text{Vs}$, and a transparency above 90 % in visible region was able to be obtained. These results indicate the promise of the present approach for making good quality ITO films at low temperature with a potential application in transparent electrode.

Acknowledgment

This work was supported by KOSEF through National Core Research Center for Nanomedical Technology (R15-2004-024-0000-0).

[References]

- [1] H. Kim, C.M. Gilmore, A. Pique, J.S. Horwitz, H. Mattoussi, H. Murata, and D.B. Chrisey, *J. Appl. Phys.* **86**, 6451 (1999).
- [2] K. Daoudi, C.S. Sandu, V.S. Teodorescu, C. Ghica, B. Canut, M.G. Blanchin, J.A. Roger, M. Oueslati, and B. Bessais, *Cryst. Eng.* **5** (2002) 187.
- [3] C.Liu, T. Matsutani, T. Asanuma, K. Murai, M. Kiuchi, E. Alves, and M. Reis, *J. Appl. Phys.* **93**, 2262 (2003).
- [4] H. Izumi, F.O. Adurodija, T. Kaneyoshi, T. Ishihara, H. Yoshioka, and M. Motoyama, *J. Appl. Phys.* **91**, 1213 (2002).
- [5] F.O. Adurodija, H. Izumi, T. Ishihara, H. Yoshioka, and M. Motoyama, *J. Mater. Sci.: Mater. Electron.* **12**, 57 (2001).
- [6] Y. Djaoued, V. H. Phong, S. Badilescu, P. V. Ashrit, F. E. Girouard, and Vo-Van Truong, *Thin Solid Films* **293**, 108 (1997).
- [7] B. E. Sernelius, K. F. Berggen, Z. C. Jin, I. Hamberg, and C. G. Granqvist, *Phys. Rev.* **B37**, 10244 (1988).
- [8] C. F. Klingshirn, *Semiconductor Optics*, Springer-Verlag Berlin Heidelberg, pp 171-173 and 248-253 (1995).

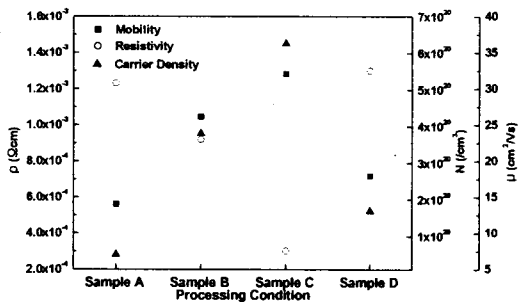


Fig.1. Variation of resistivity (ρ), carrier density (N), and Hall mobility (μ) as a function of processing conditions for ITO films. All films were grown by PLD on glass with the thickness of 200 nm.

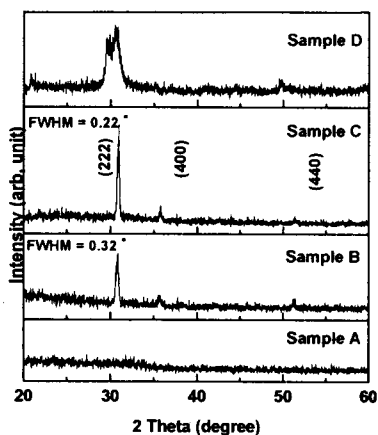


Fig.2. X-ray diffraction patterns as a function of processing conditions for ITO films deposited at room temperature. All films were grown by PLD on glass with the thickness of 200 nm.

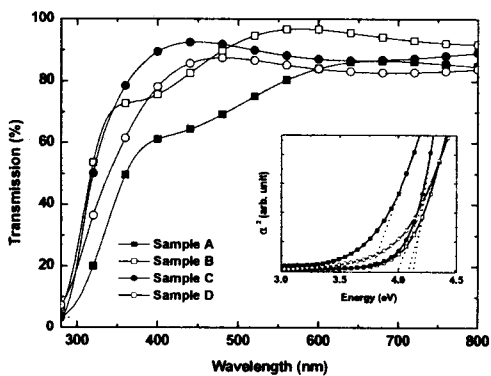


Fig.3. Effect of processing conditions on optical transmittance spectra for ITO films with an inset of optical band gap energy. All films were grown by PLD on glass with the thickness of 200 nm.